

Measurement of the kaon to pion production ratio with the Super-Kamiokande

**Tomoaki Tada,^{a,*} Yuuki Nakano,^b Yusuke Koshio^a and
for the Super-Kamiokande collaboration**

^a*Okayama University, Department of Physics,
Tsushimanaka, Kita-ku, Okayama, Japan*

^b*University of Tokyo, Kamioka Observatory, Institute for Cosmic Ray Research,
Kamioka, Hida, Gifu, Japan*

E-mail: tadatomo2976@s.okayama-u.ac.jp, ynakano@km.icrr.u-tokyo.ac.jp

Cosmic-ray muons are generated from the decay of mesons which are secondary particles produced via hadronic interaction between primary cosmic-ray particles and atmospheric nuclei at the upper the atmosphere. The mesons such pions and kaons mostly decay into muons immediately, reflecting the details of the hadronic interactions depending on their energy and lifetime. The modulation of the cosmic-ray muon rate as well as the flux and the atmospheric kaon-to-pion production ratio are important to determine the flux and energy of the atmospheric neutrino. In particular, the kaon-to-pion production ratio $r_{K/\pi}$ is measured with the correlation coefficient α_T between the cosmic-ray muon rate in the underground detector and the atmospheric temperature. As a result, we obtained the correlation coefficient $\alpha_T = 0.85 \pm 0.01$ (statistical uncertainty only) and $r_{K/\pi} = 0.12 \pm 0.03$ (statistical uncertainty only) using the data taken in 10 years at the Super-Kamiokande detector. In this article, we report the current status of measurement of the modulation of the cosmic-ray muon and the atmospheric kaon-to-pion production ratio.

38th International Cosmic Ray Conference (ICRC2023)
26 July - 3 August, 2023
Nagoya, Japan



*Speaker

1. Introduction

The framework of three-flavor neutrino mixing has been described by the Pontecorvo-Maki-Nakagawa-Sakata (PMNS) matrix [1]. The oscillation parameters have measured by various neutrino detectors. The oscillation parameter θ_{23} and Δm_{23}^2 are measured by comparing the energy spectrum of atmospheric neutrino observed in data and that of predicted by the Monte Carlo (MC) simulations. However, the uncertainty of the energy spectrum predicted by MC is dependent on the uncertainty of the absolute flux of the atmospheric neutrino. Thus, it is required to estimate the absolute atmospheric neutrino flux accurately and reduce its uncertainty. Then, using the more accurately improved MC simulations, further precise measurement of the oscillation parameters is possible.

The cosmic-ray muons are generated from the decay of mesons which are secondary particles produced via hadronic interaction between primary cosmic-ray particles and atmospheric nuclei. Since the meson such as kaon and pion are unstable, and decay into muons before interacting other particles depending on their energy and lifetime. Because the production rate of the cosmic-ray muons depends on the number of produced mesons, the muons hold essential information of the hadronic interaction. In addition, the production rate depends on the index of primary cosmic-ray energy spectra, and the profile of the upper atmosphere. When the density is low due to higher temperature, meson tends to decay into muon before interacting with the atmospheric nuclei. Such muons are likely to have high energy because they take over the energy of parent mesons. Some of these muons can reach deep underground and are observed at the underground detector. Therefore, in the high temperature season, the rate of cosmic-ray muons at the underground detector increased. Furthermore, the seasonal variation of the cosmic-ray muon rate is expected to have an amplitude which is larger than the statistical error of this rate, and correlate with the atmospheric temperature.

The study about the correlation between the muon flux and the profile of the upper atmospheric has started in 1950s [2]. An analysis method, which determines the correlation by measuring the modulation of the cosmic-ray muon rate in the underground detector, was proposed in 2010 [3]. In this method, the correlation coefficient is expressed α_T . So far a number of underground experiments have measured α_T under the various depth, and these results are good agreement with the proposed theoretical model within their estimated uncertainties. Also, the absolute flux of the atmospheric neutrino can be estimated with the measurement of the modulation of the cosmic-ray muon flux. Furthermore, the cosmic-ray muon with energy above 1 TeV has a larger contribution of the decay from kaon than that below 1 TeV. The measurement of the modulation of the cosmic-ray muon flux in the underground detector also estimate a relative contribution from kaon and pion to the cosmic-ray muon flux. The relative contribution of the decay mesons is defined as the atmospheric kaon-to-pion production ratio $r_{K/\pi}$, and this ratio is calculated using the correlation coefficient α_T . This ratio can be used as the input parameter of the atmospheric neutrino MC simulation to constraint the hadronic interaction.

For those reasons, to reduce the uncertainty of the absolute atmospheric neutrino flux and to further develop the atmospheric neutrino simulation, the precise measurement of the modulation of the cosmic-ray muon flux and the correlation with the atmospheric temperature are highly required.

2. Super-Kamiokande detector

The Super-Kamiokande detector (SK) is a water Cherenkov detector located at 1000 m underground (2700 m water equivalent) in Kamioka mine, Gifu prefecture, Japan (36.4°N and 137.3°E.) [4]. It is a cylindrical stainless steel tank, 39.3 m in diameter and 42.4 m in height, and contains 50 kiloton (ktons) of ultra-pure water. The inside of the tank is separated into an inner detector (ID) and an outer detector (OD). The ID region consists of 11,129 20-inch PMTs facing inward, and the space between the PMTs is covered with black sheet to reduce unnecessary photon reflection. A fiducial volume of the ID is defined as the cylindrical volume 2 m inward from the ID wall and has a mass of 22.5 ktons. The OD region has a width of about 2.2 m along the wall of the SK tank, it consists of 1,885 8-inch PMTs facing outward. It detects outgoing charged particles, and can also be used as a veto detector for cosmic-ray muons and low energy γ -rays from surrounding rocks. The large overburden enables to shield cosmic-ray muons, and makes the SK sensitive to cosmic-ray muons energies larger than 0.8 TeV depending on the direction. Large statistic and high muon tracking resolution are possible.

SK was started from April 1996, and now running the seventh observation phase (SK-VII). In this article, we used the data taken in the fourth phase (SK-IV), which ran from September 2008 to May 2018, and the livetime is 2,970 days.

3. The atmospheric model and the effective atmospheric temperature

For the evaluation of the correlation between the temperature of the upper atmosphere and the rate of the cosmic-ray muon observed at the underground detector, the atmospheric structure is modelled as an isothermal meson-producing entity with an effective atmospheric temperature T_{eff} [2]. This is calculated as a weighted average of the atmospheric temperature $T(X)$ corresponding to the particular atmospheric depth X . A weighted parameter $W(X)$ for calculation of T_{eff} is accounted considering the physics of the production of mesons and muons at the position corresponding to the atmospheric depth X . The effective atmospheric temperature T_{eff} is calculated using following formula,

$$T_{\text{eff}} = \frac{\int_0^{\infty} dX T(X) W(X)}{\int_0^{\infty} dX W(X)} \simeq \frac{\sum_i \Delta X_i T(X_i) W(X_i)}{\sum_i \Delta X_i W(X_i)}, \quad (1)$$

where i is the index of the discrete pressure levels. The atmospheric depth X , which has the unit of g/cm^2 , corresponds to the atmospheric pressure level by the relation $1 \text{ hPa} = 1.019 \text{ g}/\text{cm}^2$.

The correlation coefficient α_T is described as,

$$\alpha_T = \frac{T_{\text{eff}}}{R_{\mu}} \int_0^{\infty} dX W(X), \quad (2)$$

where R_{μ} is the rate of the cosmic-ray muon at the SK detector. Thus, the modulation of the cosmic-ray muon rate R_{μ} is related to that of the effective temperature T_{eff} via,

$$\frac{\Delta R_{\mu}}{\langle R_{\mu} \rangle} = \alpha_T \frac{\Delta T_{\text{eff}}}{\langle T_{\text{eff}} \rangle}. \quad (3)$$

Note that $\langle \textit{symbol} \rangle$ shows the average during the data taking period.

4. The data-set of the atmospheric temperature

We used "JRA-55" temperature data-set provided by the Japan Meteorological Agency [5]. This data-set is provided four times a day (0:00, 6:00, 12:00, and 18:00) at 37 discrete atmospheric pressure levels from 1 hPa to 1000 hPa. In addition, this is measured at each point in Japan divided by 1.25° in latitude and longitude. In this study, we used this data-set at the location of 36.25°N , 137.5°E , and its location is the closest point of the SK detector.

Figure1 shows the distribution of an average temperature at each 37 discrete atmospheric pressure levels in 10 years (from September 2008 to May 2018) corresponding to the period of the SK-IV. We calculated the effective atmospheric temperature T_{eff} based on Eq.(1). The effective atmospheric temperature T_{eff} for each day is obtained by taking the average of the four values calculated from the data-set during a day. The variance is used to estimate an uncertainty of the average of T_{eff} for every single day.

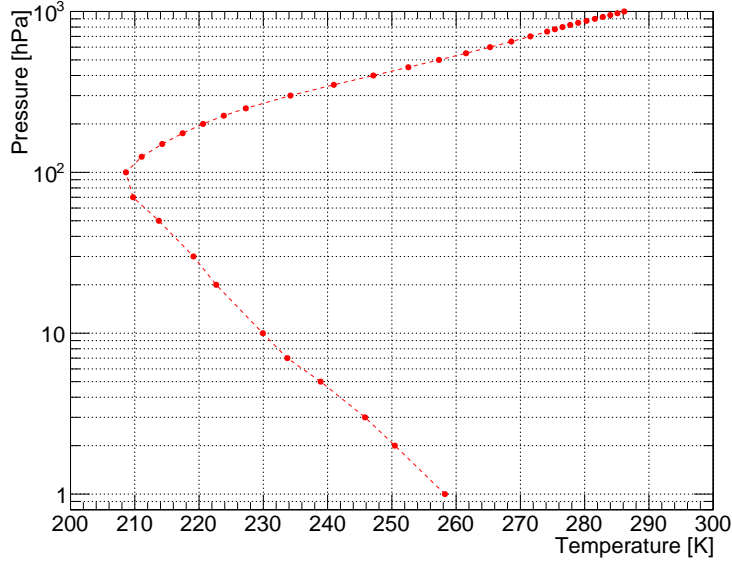


Figure 1: The distribution of an average temperature at each 37 discrete atmospheric pressure levels in 10 years corresponding to the period of SK-IV. The data-set of atmospheric temperature provided by JRA-55, and the location used this analysis is 36.25°N , 137.5°E , which is the closest point of the SK detector.

5. The reconstruction method of the cosmic-ray muon

In this article, we measured the rate of the cosmic-ray muons using the data taken in SK-IV (from September 2008 to May 2018). For the muon candidates, the total number of photoelectrons (p.e.) detected by ID PMTs is required to be greater than 1500 p.e. The muon track is reconstructed by a dedicated muon fitter called MUBOY [6, 7]. The fitter uses information from ID PMT hits, after an initial removal of noise hits, to reconstruct the muon entry point and exit point. An entry point is determined by selecting the earliest hit PMT which has at least three nearest neighbor hits within a 10 ns window. An exit point is determined by selecting the center of the nine PMTs (one

PMT and eight surrounding neighbors) which have the maximum total charge. After determining the entry and exit point, the direction of the muon track is determined.

As a result, using the muon track length and the number of the muon tracks, the muon events are reconstructed into four categories. (I) Single through-going muons: events which penetrate the ID, (II) Stopping muons: events which stopped inside the ID, (III) Multiple muons: events with several tracks, (IV) Corner clipping muons: events with a track length shorter than 7 m inside the ID. In this study, we used the muon candidates categorized as single through-going muons.

6. Result

6.1 Correlation between muon rate and the effective atmospheric temperature

We evaluate the correlation between the rate of the cosmic-ray muon R_μ and the effective atmospheric temperature T_{eff} . Figure 2 shows the deviation of the cosmic-ray muons rate R_μ and the atmospheric effective temperature T_{eff} from their overall average during 10 years corresponding to SK-IV. For the rate of the cosmic-ray muons R_μ , we counted the number of events in every single week in the Gregorian calendar which was normalized by its livetime in each week. For the atmospheric effective temperature T_{eff} , we calculated a weighted mean in every single week in the Gregorian calendar. As expected, the modulation of the cosmic-ray muon and the modulation of the effective atmospheric temperature indicate a positive correlation between the two observables (Figure 2). In order to evaluate the correlation coefficient α_T between the two observables, we performed fitting algorithm with a linear function to the data shown in Figure 2. We used the algorithm provided in CERN ROOT. Then, we obtained the correlation coefficient $\alpha_T = 0.85 \pm 0.01$ (statistical uncertainty only) of the slope of fitting function.

6.2 Calculation of the atmospheric kaon-to-pion production ratio

Kaon and pion have different masses and lifetimes, and are affected differently due to the modulation of the atmospheric temperature. Therefore, the magnitude of the correlation between the rate of the cosmic-ray muons and the atmospheric temperature depends on the kaon-to-pion production ratio $r_{\text{K}/\pi}$ in the upper atmosphere. We calculated this ratio with the results of the correlation coefficients α_T obtained in Section 6.1. The calculation method is the same as that used in Ref [8]. By considering several approximations, α_T is calculated as follows,

$$\alpha_T = \frac{1}{D_\pi} \frac{1/\epsilon_K + A_K(D_\pi/D_K)^2/\epsilon_\pi}{1/\epsilon_K + A_K(D_\pi/D_K)/\epsilon_\pi}, \quad (4)$$

with,

$$D_{\pi,K} \equiv \frac{\gamma}{\gamma + 1} \frac{\epsilon_{\pi,K}}{1.1 \langle E_{\text{thr}} \cos\theta \rangle} + 1, \quad (5)$$

where $A_K = 0.38 \times r_{\text{K}/\pi}$ is the kaon contribution to the cosmic-ray muons, $\epsilon_\pi = (114 \pm 3)$ GeV and $\epsilon_K = (851 \pm 14)$ GeV are the critical pion and kaon energies, which is the energy of the meson at which decay and interaction occur with equal probability, $\gamma = 1.70 \pm 0.01$ is the muon spectral index, $E_{\text{thr}} \cos\theta$ is the product of the threshold energy of the muon arriving at the detector and $\cos\theta$ of its zenith angle. For the Super-K site, a value of $\langle E_{\text{thr}} \cos\theta \rangle = (0.403 \pm 0.134)$ TeV

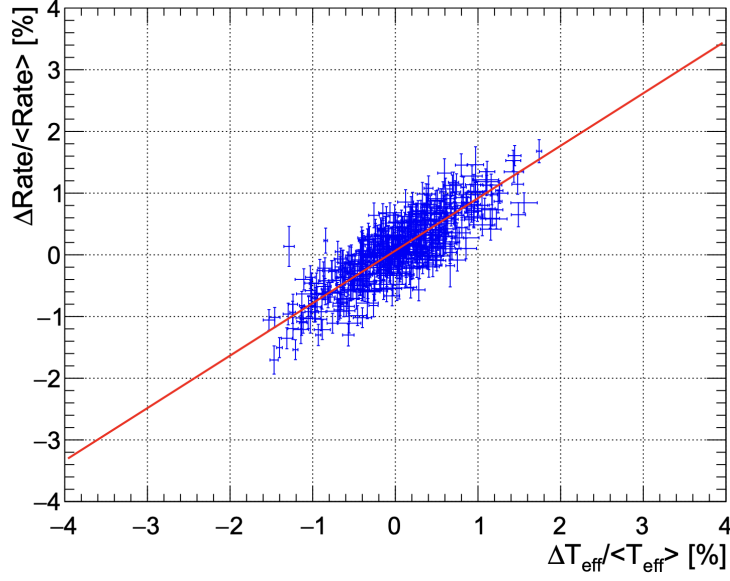


Figure 2: The scatter plot of the percent deviation of the cosmic-ray muons rate and the atmospheric effective temperature from their overall average values at the weekly binning. Red line shows the fitting linear function. We obtain $\alpha_T = 0.85 \pm 0.01$ (statistical uncertainty only) of the slope of fitting function as the correlation coefficient.

has been calculated based on MUSIC (MUon SIMulation Code : A three dimensional code for Muon Propagation through the Rock) [9, 10]. Using above formulas and the result of α_T , we got $r_{K/\pi} = 0.12 \pm 0.03$ (statistical uncertainty only) as the atmospheric kaon-to-pion production ratio.

Figure4 shows the comparison of the other measurements of the kaon-to-pion production ratio. The results of indirect measurement same as our analysis are previously presented by the several underground experiments, e.g by the MINOS [11], IceCube [12], and Borexino [8]. On the other hand, direct measurement have been performed by the several accelerator experiments, e.g. by the NA49 for the Pb + Pb collision at SPS [13], STAR for Au + Au collision at RHIC [14], and E753 for p + \bar{p} collision at Tevatron [15]. The results of the indirect measurements are placed assuming the center-of-mass energy in each experimental site. In this study, we assumed the center-of-mass energy to be $122.5^{+43.8}_{-10.0}$ GeV, which is calculated assuming the average collisions of about 8 TeV primary protons on a fixed nucleon target. The proton energy is chosen to be 10 times of the average cosmic-ray muon threshold energy $\langle E_{\text{thr}} \rangle = 0.806^{+0.670}_{-0.130}$ TeV based on MUSIC. It is assumed that cosmic-ray muons with $E > 1$ TeV have an average energy of 1/10 that of primary cosmic ray particles. The SK-IV result of the atmospheric kaon-to-pion production ratio $r_{K/\pi}$ is consistent with the other underground experiments within their uncertainty.

7. Summary

For the precise measurement of the atmospheric oscillation parameters, it is required to reduce the uncertainty of the absolute flux of the atmospheric neutrino and to constraint the hadronic interaction model in upper atmosphere. In this study, we have evaluated the correlation between the

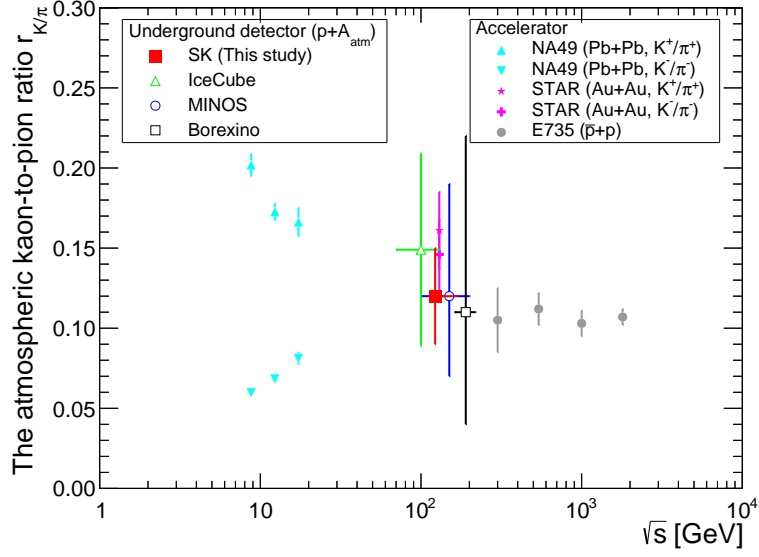


Figure 3: Comparison of several measurements of the kaon-to-pion production ratio ($r_{K/\pi}$). The red cross point shows the SK's data and other symbols with different colors show the experimental data measured by the underground detectors or accelerator experiments. NA49 and STAR experiments measured $r_{K/\pi}$ by considering the positive and negative charge separately while other experiments did without considering the charge.

modulation of the cosmic-ray muon rate observed at the SK detector and the atmospheric effective temperature T_{eff} at near the Kamioka site corresponding to SK-IV phase (from September 2008 to May 2018). As the result, we obtained the correlation coefficient $\alpha_T = 0.85 \pm 0.01$ (statistical uncertainty only). In addition, we calculated the atmospheric kaon-to-pion production ratio $r_{K/\pi}$ with the atmospheric temperature coefficient α_T , and obtained $r_{K/\pi} = 0.12 \pm 0.03$ (statistical uncertainty only). This result is consistent with the result of the other underground experiments within their uncertainties. This also provides new input information for the MC simulation.

Acknowledgments

We gratefully acknowledge cooperation of the Kamioka Mining and Smelting Company. The Super-Kamiokande experiment was built and has been operated with funding from the Japanese Ministry of Education, Science, Sports and Culture, and the U.S. Department of Energy. This work is supported by MEXT KAKENHI Grant Number 21K13942.

References

- [1] Z. Maki, M. Nakagawa and S. Sakata, *Remarks on the unified model of elementary particles*, *Prog. Theor. Phys.* **28** (1962) 870.
- [2] P.H. Barrett et al., *Interpretation of Cosmic-Ray Measurements Far Underground*, *Rev. Mod. Phys.* **24** (1952) 133.

- [3] E.W. Grashorn et al., *The Atmospheric charged kaon/pion ratio using seasonal variation methods*, *Astropart. Phys.* **33** (2010) 140 [0909.5382].
- [4] THE SUPER-KAMIOKANDE COLLABORATION collaboration, *The Super-Kamiokande detector*, *Nucl. Instrum. Meth. A* **501** (2003) 418.
- [5] Y. Harada, H. Kamahori, C. Kobayashi, H. Endo, S. Kobayashi, Y. Ota et al., *The jra-55 reanalysis: Representation of atmospheric circulation and climate variability*, *Journal of the Meteorological Society of Japan. Ser. II* **94** (2016) 269.
- [6] Z. Conner, *A study of solar neutrinos using the Super-Kamiokande detector*, Ph.D. thesis, University of Maryland, 1997.
- [7] S. Desai, *High energy neutrino astrophysics with Super-Kamiokande*, Ph.D. thesis, Boston university, 2004.
- [8] M. Agostini et al., *Modulations of the cosmic muon signal in ten years of borexino data*, *Journal of Cosmology and Astroparticle Physics* **2019** (2019) 046.
- [9] P. Antonioli et al., *A Three-dimensional code for muon propagation through the rock: Music*, *Astropart. Phys.* **7** (1997) 357 [hep-ph/9705408].
- [10] A. Tang et al., *Muon simulations for Super-Kamiokande, KamLAND and CHOOZ*, *Phys. Rev. D* **74** (2006) 053007 [hep-ph/0604078].
- [11] P. Adamson et al., *Observation of muon intensity variations by season with the minos far detector*, *Phys. Rev. D* **81** (2010) 012001.
- [12] S. Tilav, T.K. Gaisser, D. Soldin and P. Desiati, *Seasonal variation of atmospheric muons in icecube*, *arXiv preprint arXiv:1909.01406* (2019) .
- [13] THE NA49 COLLABORATION collaboration, *Energy dependence of pion and kaon production in central Pb + Pb collisions*, *Phys. Rev. C* **66** (2002) 054902 [nucl-ex/0205002].
- [14] THE STAR COLLABORATION collaboration, *Kaon production and kaon to pion ratio in Au+Au collisions at $s(NN)^{1/2} = 130$ -GeV*, *Phys. Lett. B* **595** (2004) 143 [nucl-ex/0206008].
- [15] THE E735 COLLABORATION collaboration, *Mass identified particle production in $p\bar{p}$ collisions at $\sqrt{s} = 300$ -GeV, 540-GeV, 1000-GeV, and 1800-GeV*, *Phys. Rev. D* **48** (1993) 984.

Full Authors List: Super-Kamiokande Collaboration

K. Abe,^{1,46} C. Bronner,¹ Y. Hayato,^{1,46} K. Hiraide,^{1,46} K. Hosokawa,¹ K. Ieki,^{1,46} M. Ikeda,^{1,46} J. Kameda,^{1,46} Y. Kanemura,¹ R. Kaneshima,¹ Y. Kashiwagi,¹ Y. Kataoka,^{1,46} S. Miki,¹ S. Mine,^{1,6} M. Miura,^{1,46} S. Moriyama,^{1,46} Y. Nakano,¹ M. Nakahata,^{1,46} S. Nakayama,^{1,46} Y. Noguchi,¹ K. Sato,¹ H. Sekiya,^{1,46} H. Shiba,¹ K. Shimizu,¹ M. Shiozawa,^{1,46} Y. Sonoda,¹ Y. Suzuki,¹ A. Takeda,^{1,46} Y. Takemoto,^{1,46} H. Tanaka,^{1,46} T. Yano,¹ S. Han,² T. Kajita,^{2,46,22} K. Okumura,^{2,46} T. Tashiro,² T. Tomiya,² X. Wang,² S. Yoshida,² P. Fernandez,³ L. Labarga,³ N. Ospina,³ B. Zaldivar,³ B. W. Pointon,^{5,49} E. Kearns,^{4,46} J. L. Raaf,⁴ L. Wan,⁴ T. Wester,⁴ J. Bian,⁶ N. J. Grisevich,⁶ S. Locke,⁶ M. B. Smy,^{6,46} H. W. Sobel,^{6,46} V. Takhistov,^{6,24} A. Yankelevich,⁶ J. Hill,⁷ S. H. Lee,⁸ D. H. Moon,⁸ R. G. Park,⁸ B. Bodur,⁹ K. Scholberg,^{9,46} C. W. Walter,^{9,46} A. Beauchêne,¹⁰ O. Drapier,¹⁰ A. Giampaolo,¹⁰ Th. A. Mueller,¹⁰ A. D. Santos,¹⁰ P. Paganini,¹⁰ B. Quilain,¹⁰ T. Nakamura,¹¹ J. S. Jang,¹² L. N. Machado,¹³ J. G. Learned,¹⁴ K. Choi,¹⁵ N. Iovine,¹⁵ S. Cao,¹⁶ L. H. V. Anthony,¹⁷ D. Martin,¹⁷ N. W. Prouse,¹⁷ M. Scott,¹⁷ A. A. Sztuc,¹⁷ Y. Uchida,¹⁷ V. Berardi,¹⁸ M. G. Catanesi,¹⁸ E. Radicioni,¹⁸ N. F. Calabria,¹⁹ A. Langella,¹⁹ G. De Rosa,¹⁹ G. Collazuol,²⁰ F. Iacob,²⁰ M. Mattiazzi,²⁰ L. Ludovici,²¹ M. Gonin,²² G. Pronost,²² C. Fujisawa,²³ Y. Maekawa,²³ Y. Nishimura,²³ R. Okazaki,²³ R. Akutsu,²⁴ M. Friend,²⁴ T. Hasegawa,²⁴ T. Ishida,²⁴ T. Kobayashi,²⁴ M. Jakkapu,²⁴ T. Matsubara,²⁴ T. Nakadaira,²⁴ K. Nakamura,^{24,46} Y. Oyama,²⁴ K. Sakashita,²⁴ T. Sekiguchi,²⁴ T. Tsukamoto,²⁴ N. Bhuiyan,²⁵ G. T. Burton,²⁵ F. Di Lodovico,²⁵ J. Gao,²⁵ A. Goldsack,²⁵ T. Katori,²⁵ J. Migenda,²⁵ Z. Xie,²⁵ S. Zsoldos,^{25,46} A. T. Suzuki,²⁶ Y. Takagi,²⁶ Y. Takeuchi,^{26,46} J. Feng,²⁷ L. Feng,²⁷ J. R. Hu,²⁷ Z. Hu,²⁷ T. Kikawa,²⁷ M. Mori,²⁷ T. Nakaya,^{27,46} R. A. Wendell,^{27,46} K. Yasutome,²⁷ S. J. Jenkins,²⁸ N. McCauley,²⁸ P. Mehta,²⁸ A. Tarant,²⁸ Y. Fukuda,²⁹ Y. Ito,^{30,31} H. Menjo,³⁰ K. Ninomiya,³⁰ J. Lagoda,³² S. M. Lakshmi,³² M. Mandal,³² P. Mijakowski,³² Y. S. Prabhu,³² J. Zalipska,³² M. Jia,³³ J. Jiang,³³ C. K. Jung,³³ M. J. Wilking,³³ C. Yanagisawa,^{33,1} M. Harada,³⁴ Y. Hino,³⁴ H. Ishino,³⁴ Y. Koshio,^{34,46} F. Nakanishi,³⁴ S. Sakai,³⁴ T. Tada,³⁴ T. Tano,³⁴ T. Ishizuka,³⁵ G. Barr,³⁶ D. Barrow,³⁶ L. Cook,^{36,46} S. Samani,³⁶ D. Wark,^{36,41} A. Holin,³⁷ F. Nova,³⁷ B. S. Yang,³⁸ J. Y. Yang,³⁸ J. Yoo,³⁸ J. E. P. Fannon,³⁹ L. Kneale,³⁹ M. Malek,³⁹ J. M. McElwee,³⁹ M. D. Thiesse,³⁹ L. F. Thompson,³⁹ S. T. Wilson,³⁹ H. Okazawa,⁴⁰ S. B. Kim,⁴² E. Kwon,⁴² J. W. Seo,⁴² I. Yu,⁴² A. K. Ichikawa,⁴³ K. D. Nakamura,⁴³ S. Tairafune,⁴³ K. Nishijima,⁴⁴ A. Eguchi,⁴⁵ K. Nakagiri,⁴⁵ Y. Nakajima,^{45,46} S. Shima,⁴⁵ N. Taniuchi,⁴⁵ E. Watanabe,⁴⁵ M. Yokoyama,^{45,46} P. de Perio,⁴⁶ S. Fujita,⁴⁶ K. Martens,⁴⁶ K. M. Tsui,⁴⁶ M. R. Vagins,^{46,6} J. Xia,⁴⁶ S. Izumiyama,⁴⁷ M. Kuze,⁴⁷ R. Matsumoto,⁴⁷ M. Ishitsuka,⁴⁸ H. Ito,⁴⁸ Y. Ommura,⁴⁸ N. Shigetani,⁴⁸ M. Shinoki,⁴⁸ K. Yamauchi,⁴⁸ T. Yoshida,⁴⁸ R. Gaur,⁴⁹ V. Gousy-Leblanc,^{49,2} M. Hartz,⁴⁹ A. Konaka,⁴⁹ X. Li,⁴⁹ S. Chen,⁵⁰ B. D. Xu,⁵⁰ B. Zhang,⁵⁰ M. Posiadala-Zezula,⁵¹ S. B. Boyd,⁵² R. Edwards,⁵² D. Hadley,⁵² M. Nicholson,⁵² M. O'Flaherty,⁵² B. Richards,⁵² A. Ali,^{53,49} B. Jamieson,⁵³ S. Amanai,⁵⁴ Ll. Marti,⁵⁴ A. Minamino,⁵⁴ and S. Suzuki⁵⁴

¹Kamioka Observatory, Institute for Cosmic Ray Research, University of Tokyo, Kamioka, Gifu 506-1205, Japan

²Research Center for Cosmic Neutrinos, Institute for Cosmic Ray Research, University of Tokyo, Kashiwa, Chiba 277-8582, Japan

³Department of Theoretical Physics, University Autonoma Madrid, 28049 Madrid, Spain

⁴Department of Physics, Boston University, Boston, MA 02215, USA

⁵Department of Physics, British Columbia Institute of Technology, Burnaby, BC, V5G 3H2, Canada

⁶Department of Physics and Astronomy, University of California, Irvine, Irvine, CA 92697-4575, USA

⁷Department of Physics, California State University, Dominguez Hills, Carson, CA 90747, USA

⁸Institute for Universe and Elementary Particles, Chonnam National University, Gwangju 61186, Korea

⁹Department of Physics, Duke University, Durham NC 27708, USA

¹⁰Ecole Polytechnique, IN2P3-CNRS, Laboratoire Leprince-Ringuet, F-91120 Palaiseau, France

¹¹Department of Physics, Gifu University, Gifu, Gifu 501-1193, Japan

¹²GIST College, Gwangju Institute of Science and Technology, Gwangju 500-712, Korea

¹³School of Physics and Astronomy, University of Glasgow, Glasgow, Scotland, G12 8QQ, United Kingdom

¹⁴Department of Physics and Astronomy, University of Hawaii, Honolulu, HI 96822, USA

¹⁵Institute for Basic Science (IBS), Daejeon, 34126, Korea

¹⁶Institute For Interdisciplinary Research in Science and Education, ICISE, Quy Nhon, 55121, Vietnam

¹⁷Department of Physics, Imperial College London, London, SW7 2AZ, United Kingdom

¹⁸Dipartimento Interuniversitario di Fisica, INFN Sezione di Bari and Università e Politecnico di Bari, I-70125, Bari, Italy

¹⁹Dipartimento di Fisica, INFN Sezione di Napoli and Università di Napoli, I-80126, Napoli, Italy

²⁰Dipartimento di Fisica, INFN Sezione di Padova and Università di Padova, I-35131, Padova, Italy

²¹INFN Sezione di Roma and Università di Roma "La Sapienza", I-00185, Roma, Italy

²²ILANCE, CNRS - University of Tokyo International Research Laboratory, Kashiwa, Chiba 277-8582, Japan

²³Department of Physics, Keio University, Yokohama, Kanagawa, 223-8522, Japan

²⁴High Energy Accelerator Research Organization (KEK), Tsukuba, Ibaraki 305-0801, Japan

²⁵Department of Physics, King's College London, London, WC2R 2LS, UK

²⁶Department of Physics, Kobe University, Kobe, Hyogo 657-8501, Japan

²⁷Department of Physics, Kyoto University, Kyoto, Kyoto 606-8502, Japan

²⁸Department of Physics, University of Liverpool, Liverpool, L69 7ZE, United Kingdom

²⁹Department of Physics, Miyagi University of Education, Sendai, Miyagi 980-0845, Japan

¹also at BMCC/CUNY, Science Department, New York, New York, 1007, USA.

²also at University of Victoria, Department of Physics and Astronomy, PO Box 1700 STN CSC, Victoria, BC V8W 2Y2, Canada.

- ³⁰Institute for Space-Earth Environmental Research, Nagoya University, Nagoya, Aichi 464-8602, Japan
- ³¹Kobayashi-Maskawa Institute for the Origin of Particles and the Universe, Nagoya University, Nagoya, Aichi 464-8602, Japan
- ³²National Centre For Nuclear Research, 02-093 Warsaw, Poland
- ³³Department of Physics and Astronomy, State University of New York at Stony Brook, NY 11794-3800, USA
- ³⁴Department of Physics, Okayama University, Okayama, Okayama 700-8530, Japan
- ³⁵Media Communication Center, Osaka Electro-Communication University, Neyagawa, Osaka, 572-8530, Japan
- ³⁶Department of Physics, Oxford University, Oxford, OX1 3PU, United Kingdom
- ³⁷Rutherford Appleton Laboratory, Harwell, Oxford, OX11 0QX, UK
- ³⁸Department of Physics, Seoul National University, Seoul 151-742, Korea
- ³⁹Department of Physics and Astronomy, University of Sheffield, S3 7RH, Sheffield, United Kingdom
- ⁴⁰Department of Informatics in Social Welfare, Shizuoka University of Welfare, Yaizu, Shizuoka, 425-8611, Japan
- ⁴¹STFC, Rutherford Appleton Laboratory, Harwell Oxford, and Daresbury Laboratory, Warrington, OX11 0QX, United Kingdom
- ⁴²Department of Physics, Sungkyunkwan University, Suwon 440-746, Korea
- ⁴³Department of Physics, Faculty of Science, Tohoku University, Sendai, Miyagi, 980-8578, Japan
- ⁴⁴Department of Physics, Tokai University, Hiratsuka, Kanagawa 259-1292, Japan
- ⁴⁵Department of Physics, University of Tokyo, Bunkyo, Tokyo 113-0033, Japan
- ⁴⁶Kavli Institute for the Physics and Mathematics of the Universe (WPI), The University of Tokyo Institutes for Advanced Study, University of Tokyo, Kashiwa, Chiba 277-8583, Japan
- ⁴⁷Department of Physics, Tokyo Institute of Technology, Meguro, Tokyo 152-8551, Japan
- ⁴⁸Department of Physics, Faculty of Science and Technology, Tokyo University of Science, Noda, Chiba 278-8510, Japan
- ⁴⁹TRIUMF, 4004 Wesbrook Mall, Vancouver, BC, V6T2A3, Canada
- ⁵⁰Department of Engineering Physics, Tsinghua University, Beijing, 100084, China
- ⁵¹Faculty of Physics, University of Warsaw, Warsaw, 02-093, Poland
- ⁵²Department of Physics, University of Warwick, Coventry, CV4 7AL, UK
- ⁵³Department of Physics, University of Winnipeg, MB R3J 3L8, Canada
- ⁵⁴Department of Physics, Yokohama National University, Yokohama, Kanagawa, 240-8501, Japan